Conclusion. The obtained results confirm the earlier idea [Gintov, 2005] about a strong extension of the lithosphere in the central part of the Ukrainian Shield which took place ca. 1.8 Ga ago. At this time the Shield was divided by the submeridional Kherson-Smolensk intracratonic fault belt, 60—70 km wide. The phases of transtension were interrupted by transpression phases, however extension predominated. This defined the emplacement both the Novoukrainka and Korsun'-Novomirgorod pluton.

References

Belichenko P. V., Gintov O. B Stress straine and deformation of the crustal Ukrainian Shield in the period formation of the Korsun'-Novomirgorod Pluton gabbro-anortothyte and rapakivi (tectonophysic data) // Geophys. J. — 1996. — **18**, № 2. — P. 59—69 (in Russian).

Gintov O. B. Field tectonophysics and its application for the studies of deformations of the Earth's crust of Ukraine. — Kiev: Feniks, 2005. — 572 p. (in Russian).

Gintov O. B., Orlyuk M. I., Mychak S. V., Bakarzhieva M. I., Farfuliak L. V. Subbotsko-Moshorinsky stage of the Earth's crust deformation of the Ukrainian Shield // Geophys. J. — 2008. — **30**, № 6. — P. 23—39 (in Russian).

Granitoids of the Ukrainian Shield. Petrochemistry, geochemistry, ore content. Guide / Ed. N. Scherbak. — Kiev: Nauk. dumka, 1993. — 231 p. (in Russian).

Starostenko V. I., Kazanskiy V. I., Popov N. I., Drogitskaya G. M., Zayats V. B., Makivchuk O. F., Tripolskiy A. A., Chichetov M. V. From surface structures to integral deep model of the Kirovograd ore are (Ukrainian Shield). 1 // Geophys. J. — 2010. — **32**, № 1. — P. 3—34 (in Russian).

Computer modeling of nonlinear dynamic processes in structured geophysical media

© ***S. Mykulyak, 2010***

Institute of Geophysics, National Academy of Sciences of Ukraine, Kiev, Ukraine
mykulyak@ukr.net.

In different kinds of deformation processes practically all rocks reveal specific properties such as nonlinearity, hysteresis, dilatancy and dependence on the rate of deformation. These nonlinear properties are usually attributed to the structural constitution of the materials and to the processes taking place on contacts of structural elements: crystals, grains, granules, etc. The experiments with neutron diffraction [Darling et al., 2004] confirm the dependence of the non-classical properties of sedimentary rocks (sandstones, marble and limestone) on the deformation processes of small material volumes near bonds and contacts, inhomogeneous stresses in the grains and the pore space available for grain motion. For the explicit study of this dependence the computer simulation of dynamic deformation processes in the structured medium has been performed.

The structured medium is modeled by the discrete system of 2D deformed elements (grains). Three types of grain interaction: a) elastic, b) viscoelastic and c) elastoplastic are considered. The

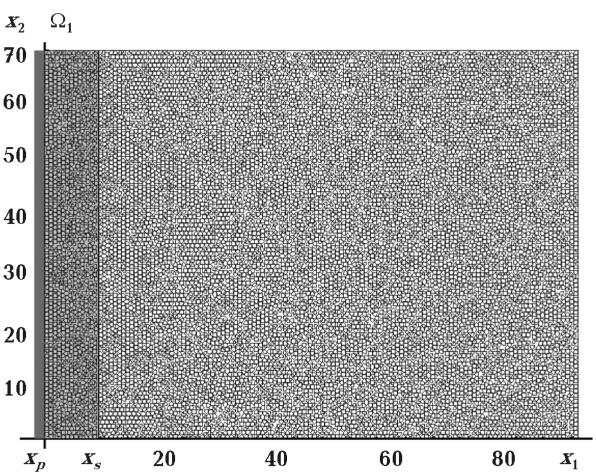

Fig. 1. The grains massif.

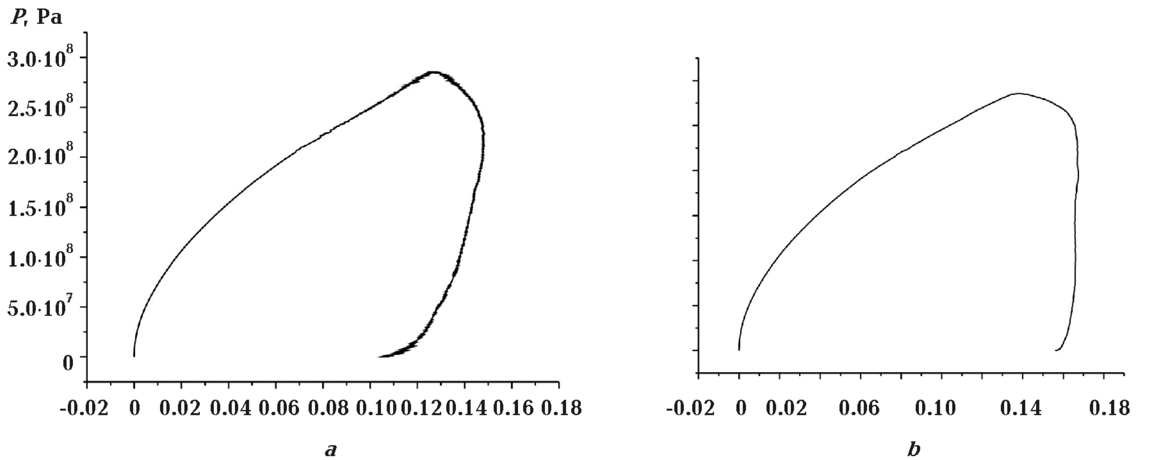

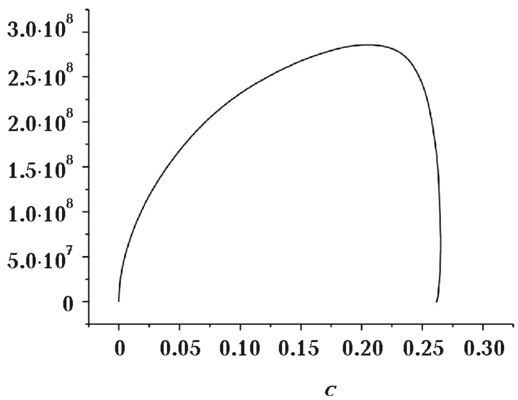

Fig. 2. The stress-strain diagrams for three types of grains interaction: *a* — elastic, *b* — viscoelastic, *c* — elastoplastic.

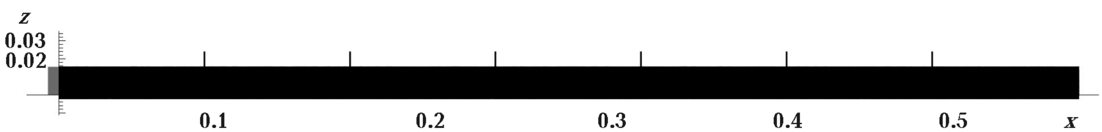

Fig. 3. The structured massif in which propagates the nonlinear wave.

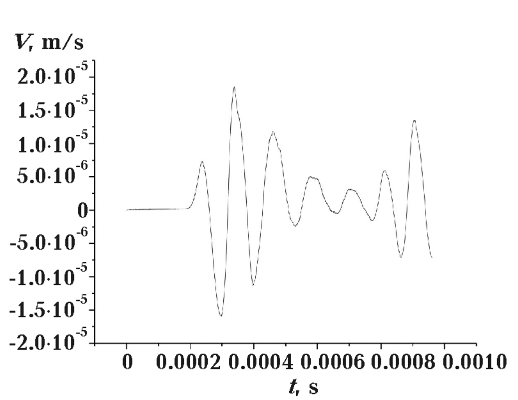

Fig. 4. Averaged velocities V_x vs. time t at the distance x=0.16.

molecular dynamic technique is used for simulation the dynamic of the discrete medium [Cundall, Strack, 1979]. The grains massif is placed in a rectangular aria (Fig. 1). The massif is deformed by the piston, which is driven by the force acting in the *x*-direction

$$f = f_0 \sin^2(\pi t / t_{\max}). \quad (1)$$

The thin wall with the coordinate x_s is located inside the massif. Knowing coordinates of piston x_p and x_s one can to determine the actual strain $\varepsilon(t)$ of the thin layer Ω_1

$$\varepsilon(t) = 1 - \frac{x_s(t) - x_p(t)}{x_s(t_0) - x_p(t_0)} \quad (2)$$

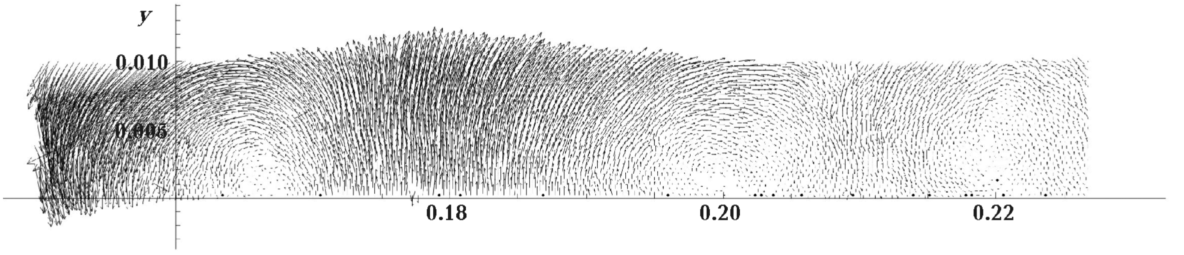

Fig. 5. The vector field at the time t=0.96 ms.

and to build the stress-strain diagram. The stress-strain diagrams for three types of grains interaction are presented in Fig. 2. All diagrams are nonlinear and hysteretic. The hysteresis squares in the viscoelastic and elastoplastic cases are greater then in the elastic one.

The second part of the report is devoted to the propagation of nonlinear wave in structured media in gravitation field. The massif consists of 56000 elements with the elastic Hertzian contacts (Fig. 3). The wave is generated by the same procedure as in the first case. Averaged mass velocities are calculated at six distances away from the piston by averaging the velocities of particles in thin layers. The dependences of the averaged velocities on time are presented in Fig. 4. The propagating wave rapidly decays being transformed then into a periodically one. Fig. 5 shows that in the massif periodical wave structures are formed. If the massif is in a prestressed state the wave attenuates slowly and the wave structures do not arise. The prestressed state is created by the z-direction weighting.

References

Cundall P. A., Strack O. D. L. A discrete numerical model for granular assemblies // Geotechnique. — 1979. — **29**, № 1. — P. 47—65.

Darling T. W., TenCate J. A., Brown D. W., Clausen B., Fogel S. C. Neutron diffraction study of grain contacts to nonlinear stress-strain behavior // Geophys. Res. Lett. — 2004. — **31**. — P. L166041—L166044.

Efficient method for solving the resistivity sounding inverse problem

© ***N. Myrontsov, 2010***

Institute of Geophysics, National Academy of Sciences of Ukraine, Kiev, Ukraine
myrontsov@ukr.net

The aim of electromagnetic sounding including the logging is to determine medium parameters on the base of measurement data. In other words, it is necessary to associate each vector $\mathbf{g}$ from the measurement space $\mathbf{G}$ to vector $\mathbf{p}$ from the space of model parameters $\mathbf{P}$. The finding of such correspondence determines the essence of solving the inverse problem.

Traditionally in solving the logging inverse problem, it is accepted to use a minimization of the functional:

$$F\left(\rho_1^T,...,\rho_n^T\right)=\sqrt{\sum_{i=1}^{n}\left(\frac{\rho_i^T-\rho_i^P}{\delta_i\rho_i^T}\right)^2}\ , \qquad (1)$$

where: n is the number of sounds in the equipment, ρ_i^T are computed theoretical values of apparent resistance (AR) of the model under consideration, ρ_i^P are values obtained really in AR measuring and δ_i is the value of error for i-th sound. The values of model parameters, to which computed ρ_i^T correspond at each step of the iterative process of minimization of